JOURNAL OF MATERIALS SCIENCE 20 (1985) 3771–3777

The near-surface structure of ion-implanted and crept molybdenum

I. W. HALL
Department of Mechanical Engineering, University of Delaware, Newark, Delaware 19716, USA

Transmission electron microscope specimens have been prepared from the surface of ion-implanted and crept molybdenum sheet. The structure of the near-surface layers is found to be very strongly influenced by the type of implanted ion species and the implantation energy. Creep of carbon-implanted specimens produced, within the subgrains, a high density of jogged dislocations upon which precipitation had occurred. Creep of tellurium-implanted specimens led to the production of large numbers of voids close to the specimen surface; precipitation was frequently noted in conjunction with the voids. Voids were observed particularly in the grain boundaries. Examination of crept samples in the scanning electron microscope showed that grain boundary sliding was of importance in tellurium-implanted samples. The observations are considered in terms of the diffusion of interstitial carbon and radiation-induced defects.

1. Introduction

Ion implantation is a widely used research tool for the investigation of radiation damage processes and fundamental precipitation and solubility effects [1–3]. As a practical tool to aid the metallurgist, its use has been limited mainly to providing surface coatings for increased wear resistance and oxidation or corrosion resistance [4–6]. There has, so far, been little evidence that ion implantation can seriously affect what may be termed "bulk" properties. However, recent work has shown that the creep resistance of thin sheet molybdenum can be dramatically affected by implantation with various ion species [7]. Briefly, it was found that implantation with heavy substitutional atoms could cause a decrease in creep resistance whilst implantation with lighter interstitial atoms was capable of producing very great increases in creep resistance. These general trends were altered if heat treatments were carried out between the initial implantation step and the creep test. The heat treatments investigated consisted of high-temperature anneals, carried out at temperatures between 900 and 1200° C.

The previous work investigated the effects of ion implantation and annealing on thin foils. The work reported here was initiated in order to permit direct observation of the microstructure present in the surface layers after creep testing. By this means the validity of the earlier observations would be investigated and the causes of the phenomenon would be clarified.

2. Experimental methods

Thin, pure molybdenum sheet creep specimens 200 μm in thickness were implanted on both surfaces with either carbon ions at 60 keV or tellurium ions at 350 keV. The projected ranges of these ions are 63 nm and 49 nm, respectively [8], and the doses chosen were sufficient to yield an implanted layer containing 4 at % carbon or 2 at % tellurium. Complete details concerning the implantations and the preparation and testing of the creep specimens can be found in an earlier paper [7]. Some of these specimens have been examined in the scanning electron microscope (SEM) in order to characterize the final fracture mode and to determine whether any gross differences in surface appearance were

0022–2461/85 $03.00 + .12 © *1985 Chapman and Hall Ltd.*

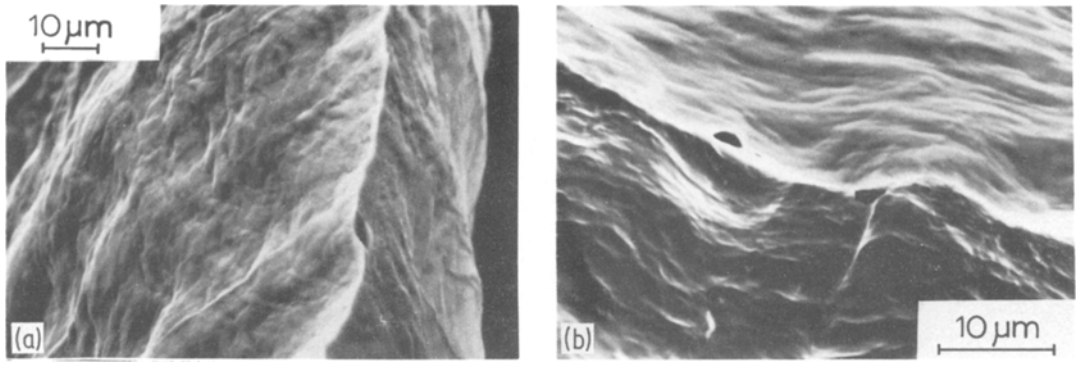

Figure 1 Fracture surfaces of (a) unimplanted sample and (b) tellurium-implanted sample.

developed during creep testing which might be attributable to the effects of ion implantation.

Specimens for transmission electron microscopy (TEM) were prepared as 3 mm diameter discs and examined at 120 kV in a Philips EM 400T Scanning Transmission Electron Microscope. These specimens were prepared by trepanning discs from the 200 μm thick creep specimens; some were then electropolished uniformly from both sides. Other samples were prepared by masking one side of the disc with a layer of wax and then carrying out the usual jetting and polishing process on the exposed side alone. By using this method the final perforation of the foil was located in the surface layer of the specimen. Needless to say, the quality of thin foils prepared in this way from samples which have been crept to failure at high temperature is not quite as good as that of conventionally produced foils: nevertheless, the observations made on these foils confirm beyond doubt that this method is successful in preserving the surface layer.

3. Experimental results

The fracture surfaces of all the creep specimens were essentially identical and in each case final fracture had occurred by necking down to a knife edge. Figs. 1a and b show the fracture surfaces of an unimplanted sample and a tellurium-implanted sample, respectively. Voids were occasionally observed to have nucleated along these knife edges but the principal feature of all these surfaces was that pronounced slip lines were clearly developed.

Examination of the surface of the crept samples at a position more than 100 μm from the final fracture confirmed that extensive plastic deformation had occurred. First, slip lines were very well developed in all the grains. Secondly, the grain size was easily discernible due to the effect of grain boundary sliding (GBS). However, significant differences were also noted between the specimens with respect to the extent of GBS that had occurred. GBS was most evident in specimens implanted with tellurium and offsets of several micrometres were quite commonly

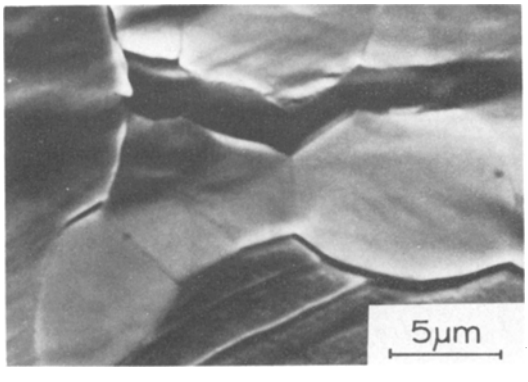

Figure 2 Evidence of grain boundary sliding in tellurium-implanted and crept sample.

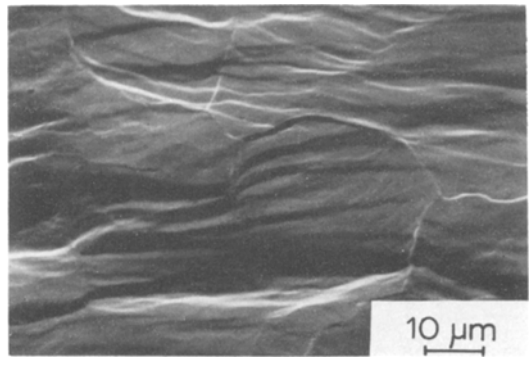

Figure 3 Surface of carbon-implanted and crept sample showing wavy slip lines and no evidence of grain boundary sliding.

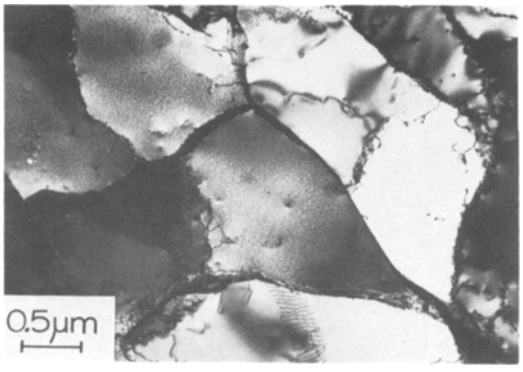

Figure 4 Micrograph from the mid-thickness of an unimplanted and crept sample showing clearly developed cell structure with strain-free interiors.

observed (Fig. 2). Unimplanted samples showed comparatively much less evidence of GBS.

The surfaces of specimens implanted with carbon exhibited very little evidence of GBS after the creep tests. The elongations recorded for these samples were considerably greater than those for unimplanted or tellurium-implanted specimens, yet all the plastic deformation had been accommodated by the more conventional modes of plastic deformation, as evidenced by the slip lines on the surfaces (Fig. 3).

Specimens examined in the TEM showed much greater diversity in structure. Unimplanted specimens crept at temperatures up to 1100° C had developed well defined subgrains, approximately 0.1 μm in diameter. The appearance and size of these subgrains were independent of the position of the specimen from which the foil was prepared, i.e. mid-thickness, surface, etc. The interiors of the subgrains were almost free of dislocation debris and no evidence of any precipitation or vacancy condensation reaction was found. A typical unimplanted and crept specimen is shown in Fig. 4.

Carbon-implanted samples were examined next and it was found that foils from the mid-thickness of creep specimens exhibited practically the same microstructures as unimplanted samples. However, foils from the surface of carbon-implanted and crept samples were much different. The subgrains present in these foils were less well defined than their counterparts in unimplanted samples and their interiors generally contained a large amount of dislocation debris. Closer examination of this debris showed that the dislocations had been subjected to very heavy pinning, and most were heavily jogged (Fig. 5a). In addition, many dislocation loops with an average diameter of approximately 25 nm are visible in the grain interiors. Fig. 5b shows a higher magnification view of such a region in which actual precipitates are seen (arrowed) on the dislocations; these are believed to be carbides but it was not possible unambiguously to identify them by electron diffraction.

The mid-thickness regions of tellurium-implanted and crept specimens were indistinguishable from those of unimplanted specimens. The near-surface foils were unique. The main feature of these foils was the appearance of enormous numbers of voids, ranging in size from approximately 20 to almost 200 nm (Fig. 6). Stereomicroscopy was employed to determine the density of voids and, whilst the counting of the smaller voids may be somewhat

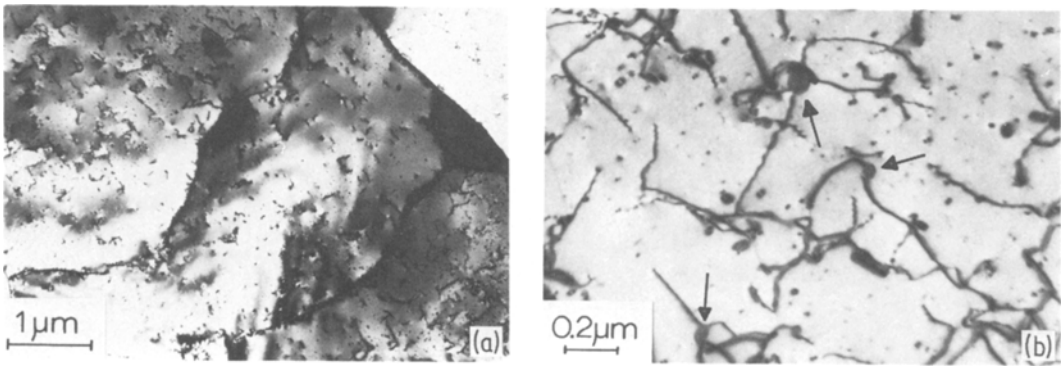

Figure 5 (a) Foil from the surface of carbon-implanted and crept sample showing jogged and pinned dislocations with other debris within the subgrains. (b) As (a) but showing precipitates (arrowed) on dislocations.

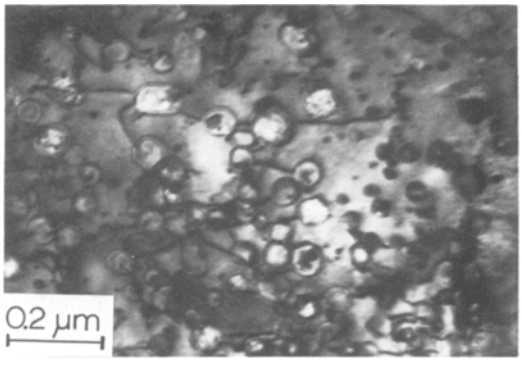

Figure 6 Foil from the surface of a tellurium-implanted and crept sample showing high concentration of voids.

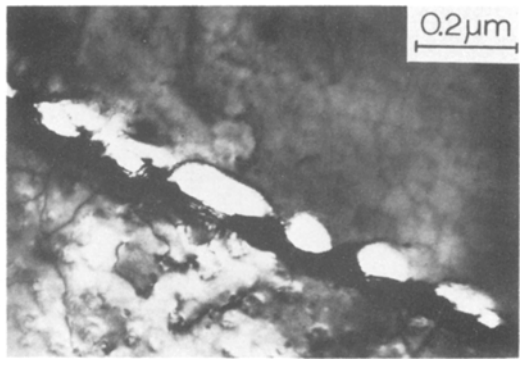

Figure 8 Voids in grain boundary of a tellurium-implanted and crept sample.

subjective, it can be conservatively estimated that there were approximately $10^{16}\,cm^{-3}$ in those regions of highest density. Stereomicroscopy showed that these voids were distributed randomly within the observable thickness of the foil and were not concentrated at any particular depth.

The voids generally appeared as multifaceted spheres, although occasional elongated ones were noted, probably indicating that two voids had just coalesced and were in the process of reducing their surface area/volume ratio. The voids were commonly noted to have nucleated along, and thus be linked by, dislocation lines. It was further noted that many of the voids were associated with a precipitate particle. These are seen as small black cubes and are clearly shown in Fig. 7. Although it was not possible to obtain micro-microdiffraction patterns from these particles, energy-dispersive X-ray analysis showed them to be tellurium-rich when compared to the matrix. Quantitative analysis of such a particle is impossible since the analysing beam also penetrates an unknown thickness of matrix and the amount of beam spreading cannot be accurately determined.

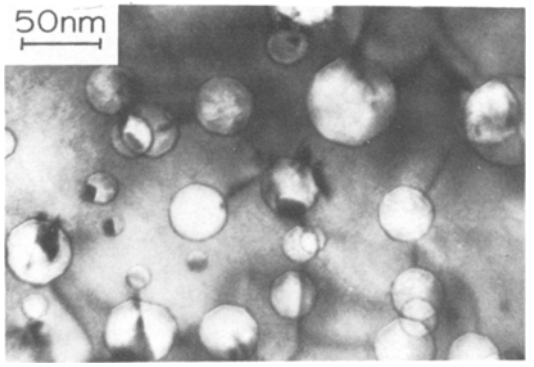

Figure 7 Micrograph showing faceted appearance of voids as well as their frequent association with cuboid precipitates and dislocation lines.

Voids were also found on grain boundaries where they assumed a more lenticular shape as would be expected from surface energy considerations. This behaviour is illustrated in Fig. 8.

4. Discussion

If the results of the present work are considered in conjunction with previous observations of the same material systems, several significant differences are at once apparent. Molybdenum specimens implanted with the same ions but not subjected to any creep testing have been examined before in the electron microscope [7]: in this previous study high-temperature annealing treatments were employed in an attempt to simulate the thermal effects that might occur during creep testing. Specimens used in that study were foils already thinned for examination in the TEM before being implanted. They were thus much thinner than the creep specimens used here even though they were approximately four times thicker than the projected range of the most energetic ions used. That study showed that carbon implantation and annealing led to the formation of fine dendritic precipitates and that tellurium implantation and annealing led to the formation of small cubic particles. However, the present work now makes it clear that the morphology of precipitate particles is strongly dependent upon the plastic strain that occurs during creep. In particular, in the present study,

carbon-implanted specimens showed no evidence that dendritic precipitates had occurred during creep, whereas they had been found in annealed but uncrept thin foils. Tellurium-implanted and crept samples showed voids in much greater numbers than were ever seen in uncrept samples. They also exhibited cuboid-shaped precipitates similar to those observed before. These differences in precipitation behaviour require explanation. Furthermore, any explanation of the effects of ion implantation on the creep resistance must be able to explain satisfactorily how an implanted layer that constitutes less than 0.04 to 0.08% of the volume of the sample can cause more than a 2000% increase or more than a 1500% decrease in this property [7]. These effects of implantation, annealing and creep testing are intimately related to the redistribution of the implanted solute elements and the simultaneously produced point defects. It is thus instructive to consider the extent and consequences of the diffusion of these species, beginning with carbon. In carbon-implanted samples, the excess vacancy concentration is believed to be of minor importance, when compared to the effect of interstitial carbon, since implantation was carried out at a low accelerating voltage and radiation damage was thus limited. Also, interstitial carbon is much more mobile than are molybdenum vacancies.

The absence of the relatively large dendritic carbide precipitates in carbon-implanted and crept specimens indicates either that local supersaturation of carbon close to the surface could be relieved by diffusion into the bulk or that sufficient nucleation sites existed to maintain a very small average precipitate size indeed, probably less than 2 nm. Diffusion of excess carbon into the bulk was not a possibility for implanted thin foils and, also, the means for rapid mass transfer were not available in the form of a high density of dislocations. Using Rudman's data for the diffusivity and solubility of carbon in molybdenum [9], the diffusivity is given by an expression of the form

$$D = 0.034 \exp(-41\,000/RT)$$

and the solubility of carbon may be estimated to be less than 10^{-3} at % at 1000° C. As stated above, the carbon concentration within the implanted layer was approximately 4 at %. Let us consider firstly the case of implanted thin foils. In order to estimate the time necessary for the carbon concentration to exceed the solid solubility throughout the foil, it is assumed that diffusion only occurs perpendicularly to the surface and that the implanted surface layer provides a thin, non-depletable source of carbon. The equation used for carburization calculations, namely

$$C(x, t) = C_s - (C_s - C_0)\,\mathrm{erf}(x/2\sqrt{Dt})$$

(C_s is the surface concentration and C_0 is the original concentration in the bulk, assumed to be zero here), can be used to give an estimate of the time required for the concentration at the opposite foil surface to reach 99% of the solubility limit. It is found that this occurs after less than 400 sec at 1000° C and hence precipitates are readily visible throughout these foils, even after very short annealing times.

Next, consider the case in which carbon diffuses from a 60 nm thick implanted layer into the mid-thickness of a 200 μm thick creep sample. Utilizing the graphical solution given by Crank [10] for diffusion into a plane sheet of thickness 200 μm from two surfaces whose concentrations are 10^{-3} at %, the carbon concentration at a depth of 20 μm, for example, will be greater than 95% of the solid solubility after approximately 15 min. Thus, precipitation would be expected at appreciable depths after quite short times at high temperature. Furthermore, the presence of large numbers of moving dislocations, as demonstrated by the slip lines on the surface, will greatly enhance pipe diffusion, reducing this time significantly. The same dislocations will provide abundant nucleation sites for precipitation, thus ensuring that no large dendritic precipitates are formed. A further feature of the crept samples is that they were polycrystalline with a grain size of approximately 10 μm. Not only would the grain boundaries provide easier diffusion paths, but they would also provide sites for nucleation of precipitates. The absence of the previously observed dendritic precipitates can thus be explained by consideration of the diffusion of carbon and the availability of nucleation sites.

The diffusion of carbon as outlined above would lead to copious fine-scale precipitation within an appreciable volume of the sample. Consequently, the strengthening effect of these precipitates would be noted not only within the implanted layer but also throughout much of the

sample volume. In this manner, much of the sample would be subjected to a strain ageing phenomenon which is capable of increasing the creep resistance. The creep test data confirm that increases in creep resistance are most marked in tests where no annealing step has been interposed between implantation and creep testing. In those cases where an annealing treatment was used there was no marked increase in creep resistance since stable precipitates had formed and no strain ageing effect occurred.

A similar approach may be used to account for the occurrence of the large number of voids in tellurium-implanted and crept specimens. One of the major effects of heavy-ion implantation is to introduce a large number of point defects: the highly mobile self-interstitials will rapidly anneal out but the vacancies generated will persist for longer times and thus be able to exert a significant influence upon the development of the microstructure after implantation and during the early stages of creep. The vacancy concentration present in the surface layer after implantation can only be estimated approximately, since there is no way of accurately accounting for the number of vacancies that leave the surfaces of the foil during the so-called thermal spike. However, an estimate of a vacancy concentration of 10^{-4} has been made [7] using the simple Kinchin and Pease [11] equation. It is also possible to estimate C_v, the equilibrium vacancy concentration, at 1000° C either by assuming it to be about 10^{-4} at the melting point (as is the case for most metals) or by assuming the enthalpy of formation of a mole of vacancies to be approximately half of the activation energy for self-diffusion (as is also the cae for many metals). The latter is known to be 460 kJ mol^{-1} [12]. Using either of these estimates, C_v at 1000° C is found to be in the range 10^{-9} to 10^{-10}. There is thus a supersaturation of vacancies which has several effects upon the microstructure as it anneals out. First, the large flux of vacancies is sufficient to cause migration of grain boundaries [13]. Secondly, in thin foils a large number of dislocation loops is formed as the vacancies coalesce and collapse to form planar defects [13]. In thin foils the two free surfaces close to the implanted layer provide an easily accessible sink for the excess vacancies and voids were rarely found. However, in the thicker creep specimens, many of the vacancies will have diffused into the bulk of the sample or will have been swept up by the moving dislocations and begun to nucleate the voids which are seen to form a "necklace" on the dislocations in Figs. 6 and 7.

One significant difference between the cases of vacancy diffusion here and interstitial carbon diffusion considered above is that the vacancies will be annihilated at grain boundaries whilst interstitial carbon atoms will not. Hence, any effect due to vacancies should only be noticeable within one grain diameter of the surface. In these creep specimens with a grain size of 10 μm it is thus possible that 10% of the volume of the sample contained a vacancy concentration greatly in excess of the usual thermodynamically stable concentration. This vacancy concentration would obviously decrease, but could only do so relatively slowly when compared with the speed at which the concentration of interstitial carbon can change. During the time in which C_v is approaching its normal value the creep mechanisms that occur are those which generally occur at much higher temperatures, where the normal C_v is much higher. Thus, for example, Herring–Nabarro or Coble creep may occur. The strength of this 10 μm layer on each surface would be negligible when compared with that of the mid-thickness material. Applying the usual power law of the form:

$$\dot{\varepsilon} = A\sigma^n \exp(-Q/RT)$$

to creep of molybdenum, the effect of a 10% decrease in cross-sectional area would increase the stress and thus the creep rate. For an exponent $n = 5$ the increase in creep rate could be 70%.

The experimental data are in broad agreement with the interpretation. In addition, the observation of voids nucleated along grain boundaries (Fig. 8) and extensive GBS in tellurium-implanted and crept samples (Fig. 2) is a strong indicator that Coble creep, which requires a high value of C_v, had occurred. Annealing, either for extended periods or at high temperatures, after implantation and before creep testing allowed the vacancy concentration to equilibrate again and no change was noted in mechanical properties. In this case, the precipitates formed were large and the solute was not mobile enough to give rise to a strain ageing effect.

Whilst the current rationale for the effects of

implantation can explain the general trends, it is quite clearly insufficient to account in detail for the magnitude of the effects, e.g. a reduction in creep resistance of 70% has been calculated for tellurium-implanted samples but the actual reduction was more than 1500%. It is to be concluded, therefore, that the foregoing discussion provides only a partial explanation of the phenomenon and much work needs to be done to clarify it totally.

In summary, the experimental observations reported here support the view that light-ion implantation can give rise to significant strain ageing effects and that heavy-ion implantation can cause decreased creep resistance due to the radiation damage introduced. In the latter case, the effect should be limited in extent by the grain size of the sample; the larger the grain size, the deeper the vacancies may penetrate. The importance of these results lies in the demonstration that radiation damage to the surface of a stressed sample, however caused, cannot be assumed to be innocuous simply because the sample dimensions are large compared with the thickness of the damage layer. Also, this phenomenon shows that radiation damage produced in a single limited exposure can affect creep resistance: this is in contrast to the more widely known and investigated phenomenon of radiation-enhanced creep, where creep rates are affected only while the irradiation treatment is in progress and damage is accumulating. Much further work is required to delineate the possible extent of this phenomenon.

References

1. J. H. EVANS, D. J. MAZEY, B. L. EYRE, S. K. ERENTS and G. M. McCRACKEN, "Applications of Ion Beams to Materials", Institute of Physics Conference Series 28 (Institute of Physics, Bristol, 1975) p. 229.
2. J. A. HUDSON, R. J. McELROY and R. S. NELSON, *ibid.*, p. 251.
3. R. S. NELSON, "Applications of Ion Beams to Metals", edited by S. T. Picraux, E. P. EerNisse and F. L. Vook (Plenum, New York, 1974) p. 221.
4. Proceedings of Conference on Ion Implantation and Ion Beam Analysis in Corrosion Studies, Manchester, *Corr. Sci.* **16** (1976).
5. J. D. BENJAMIN and G. DEARNALEY, "Applications of Ion Beams to Materials", Institute of Physics Conference Series 28 (Institute of Physics, Bristol, 1975) p. 141.
6. N. E. W. HARTLEY, "Treatise on Materials Science and Technology", edited by J. K. Hirvonen (Academic Press, New York, 1980) p. 321.
7. I. W. HALL, *Met. Trans.* **12A** (1981) 2093.
8. B. SMITH, "Ion Implantation Range Data for Silicon and Germanium Device Technologies" (Research Studies Press, Oregon, 1977).
9. P. S. RUDMAN, *Trans. Met. Soc. AIME* **239** (1967) 1949.
10. J. CRANK, "The Mathematics of Diffusion" (Oxford University Press, London, 1957) p. 46.
11. G. H. KINCHIN and R. S. PEASE, *Rep. Prog. Phys.* **17** (1955).
12. A. M. BROWN and M. F. ASHBY, *Acta Metall.* **28** (1980) 1085.
13. I. W. HALL, *Radiat. Eff.* **61** (1982) 165.

Received 22 October
and accepted 10 December 1984